Supplemental data

TABLE OF CONTENTS

1. Supplemental Figure legends

Supplemental Figure 1. Expression of macrophage markers in SVF from HFD mice.

(**A**) Expression of macrophage marker genes in isolated stromal-vascular fraction (SVF) of adipose tissue (eWAT and iWAT) from chow and HFD fed mice by qPCR. (**B**) SVF isolated from eWAT and iWAT of chow and HFD fed mice were gated for live $CD45^+$ cells. Representative scatter-plot showing macrophages stained with F4/80 and CD11b antibody. (**C** and **D**) Expression of *Irf3* and macrophage marker genes in sorted $F4/80^+$ $CD11b^+$ macrophages by FACS. n=5-6/group. Data is presented as mean ± SEM. For all data, *p<0.05.

Supplemental Figure 2. Effect of LPS, palmitate and poly I:C treatment in the absence or presence of IRF3.

(**A**) Expression of mouse IRF3 at mRNA and protein level in mature 3T3-L1 adipocytes transduced with lentivirus expressing shRNA against mouse Irf3, determined by qPCR and Western blotting. n=4. (**B**) Western blot showing effect of LPS treatment on protein levels of p65 and phospho-p65 in isolated nuclei and/or cytosolic fraction of 3T3-L1 adipocytes. (**C**) Effect of LPS (700 ng/ml) treatment for 6 days on NF-κB activity in the isolated nuclei fraction from 3T3-L1 adipocytes using TransAm NF-κB activity kit. Lysate from Raw 264.7 cells treated with LPS (700 ng/ml) for 1 h was used as a positive control. (**D**) Basal and insulin-stimulated glucose uptake in 3T3-L1 adipocytes after treatment with varying doses of palmitate for 48 h. (**E**) Basal and insulin-stimulated glucose uptake in 3T3-L1 adipocytes transduced with lentivirus expressing shRNA against Irf3 or shLuc control hairpin in the absence or presence of palmitate treatment (1 mM). (**F**) Western blot showing effect of poly I:C treatment on protein levels of p65 and phospho-p65 in isolated nuclei and/or cytosolic fraction of 3T3-L1 adipocytes. Data is presented as mean ± SEM. ***p<0.001, **p<0.01, *p<0.05.

Supplemental Figure 3. Effect of IRF3 overexpression on insulin signaling in 3T3-L1 adipocytes.

(**A**) Schematic representation of the wild-type IRF3 and mutant IRF3 (IRF3-2D) protein. (**B**) Overexpression of mouse IRF3 and IRF3-2D mutant at mRNA and protein level in mature 3T3-L1 adipocytes transduced with lentivirus, determined by qPCR and Western blotting. n=4. (**C**) Effect of IRF3 overexpression on inflammatory gene expression by lentivirus transduction in mature 3T3-L1 adipocytes using qPCR. n=4. (**D**) Effect of IRF3 overexpression on insulin signaling in mature 3T3-L1 adipocytes by Western blotting. Data is presented as mean ± SEM. **p*<0.05, ****p*<0.001.

Supplemental Figure 4. Differentially regulated genes by IRF3 overexpression or knockdown in the absence or presence of LPS.

(**A**) Heat map showing gene expression fold change between three groups (IRF3-2D vs EGFP, shIrf3 vs shLuc, and shIrf3 vs shLuc in the presence of LPS). Scale is log2 fold change. (**B**) Effect of IRF3 overexpression in mature 3T3-L1 adipocytes on insulin signaling genes from Cluster 2 of RNA-seq, validated by qPCR. Data is presented as mean ± SEM. **p*<0.05 (**C-F**) Number of upregulated or downregulated genes by IRF3 expression between five groups (IRF3-2D vs EGFP, shIrf3 vs shLuc, shLuc vs shLuc in the presence of LPS, shIrf3 vs shIrf3 in the presence of LPS, and shIrf3 vs shLuc in the presence of LPS).

Supplemental Figure 5. Characteristics of *Irf3*$^{-/-}$ mice on chow diet.

(**A**) Expression of IRF3 target inflammatory genes in eWAT by qPCR. (**B**) Plasma cytokine levels measured in *Irf3*$^{-/-}$ mice. (**C**) Body weight of WT and *Irf3*$^{-/-}$ mice. (**D**) Body composition determined in *Irf3*$^{-/-}$ mice. All data from male chow-fed 16 week old control and *Irf3*$^{-/-}$ mice, n=6-7/genotype. Data is presented as mean ± SEM. For all data, **p*<0.05.

Supplemental Figure 6. Effect of Irf3 deficiency on insulin sensitivity in chow and HFD fed mice.

(**A**) Glucose tolerance test (GTT) in *Irf3*$^{-/-}$ mice after 8 weeks on chow diet. (**B**) Insulin tolerance test (ITT) in *Irf3*$^{-/-}$ mice after 10 weeks on chow diet. (**C**) Fasting plasma glucose levels in *Irf3*$^{-/-}$ mice after 8 and 10 weeks on HFD. (**D**) Western blot showing insulin signaling in eWAT of *Irf3*$^{-/-}$ mice on HFD. (**E**) Quantification of Western blot in Supplemental Figure 6D. (**F**) Western blot showing insulin signaling in liver of *Irf3*$^{-/-}$ mice on HFD. (**G**) Quantification of Western blot in Supplemental Figure 6F. N=6-7/genotype for chow studies. N= 7-8/genotype for HFD studies. Data is presented as mean ± SEM. For all data *p<0.05.

Supplemental Figure 7. Hyperinsulinemic-euglycemic clamp in *Irf3*$^{-/-}$ mice on HFD.

(**A**) Fasting and clamped glucose levels in control and *Irf3*$^{-/-}$ mice after 8 weeks of HFD feeding. (**B**) Fasting and clamped insulin levels in control and *Irf3*$^{-/-}$ mice. (**C**) Fasting and clamped non-esterified fatty acids (NEFAs) levels in control and *Irf3*$^{-/-}$ mice. For all data N=8-10 per genotype. Data is presented as mean ± SEM.

Supplemental Figure 8. Effect of Irf3 deficiency on Glut4 and adiponectin levels in HFD fed mice.

(**A**) Adiponectin (*Adipoq*) mRNA levels in 3T3-L1 adipocytes following overexpression or knockdown of IRF3 by qPCR. (**B**) Expression of *Adipoq* in eWAT and iWAT of WT and *Irf3*$^{-/-}$ mice on HFD by qPCR. (**C**) Plasma adiponectin levels in WT and *Irf3*$^{-/-}$ mice on HFD. (**D**) Glut4 protein levels in eWAT and iWAT of chow vs HFD mice determined by Western blotting. (**E**) Gene expression of *Slc2a4* in 3T3-L1 adipocytes with overexpression and knockdown of murine IRF3. N=4 for in vitro studies. N= 7-8/genotype for HFD studies. Data is presented as mean ± SEM. For all data *p<0.05.

Supplemental Figure 9. Energy expenditure and expression of thermogenic genes in BAT of *Irf3*$^{-/-}$ mice on HFD.

CLAMS study was performed on *Irf3*$^{-/-}$ mice upon 16 weeks of HFD feeding to determine effect on (**A**) food intake, (**B**) activity, (**C**) respiratory exchange ratio (RER), and (**D**) heat production. (**E**) Histology showing H&E staining in BAT of *Irf3*$^{-/-}$ mice on HFD (10X magnification). (**F**) Expression of thermogenic and β-oxidation genes in BAT of *Irf3*$^{-/-}$ mice on HFD. For all data n=7-8/genotype. Data is presented as mean ± SEM. For all data, **p*<0.05.

Supplemental Figure 10. Energy expenditure and expression of thermogenic genes in BAT of *Irf3*$^{-/-}$ mice on HFD before body weight divergence.

Male wild-type and *Irf3*$^{-/-}$ mice were fed HFD and used for CLAMS study. N=6/genotype. (**A**) Body weight of WT and *Irf3*$^{-/-}$ mice during 10 weeks HFD feeding. (**B**) Body composition of WT and *Irf3*$^{-/-}$ mice at 8 weeks of HFD feeding. (**C**) Tissue weight of WT and *Irf3*$^{-/-}$ mice after 10 weeks on HFD. (**D**) Food intake, (**E**) activity, (**F**) respiratory exchange ratio (RER), and (**G**) heat production in *Irf3*$^{-/-}$ mice upon 8 weeks of HFD. (**H**) Histology showing H&E staining in BAT of *Irf3*$^{-/-}$ mice upon 10 weeks of HFD (10X magnification). (**I**) Expression of thermogenic and β-oxidation genes in BAT of *Irf3*$^{-/-}$ mice upon 10 weeks of HFD. Data is presented as mean ± SEM. For all data **p*<0.05.

2. Supplemental Table Legends

Supplemental Table 1. Human subjects characteristic and plasma parameters.

Supplemental Table 2. List of genes coordinately regulated by overexpression and knock-down of murine IRF3. Numbers represent log2 fold change with ≤25% FDR.

Supplemental Table 3. Top pathways enriched in the three major clusters identified in Figure 3B by GSEA using DAVID.

Supplemental Table 4. List of pathways regulated in clusters identified in Figure 3B with ≤25% FDR.

Supplemental Table 5. Plasma parameters of *Irf3*$^{-/-}$ mice on chow and high-fat diet. Plasma samples were collected from 16 week old male *Irf3*$^{-/-}$ mice on chow and high-fat diet (HFD) in the fed state. Data is represented as mean ± SEM. N=6-7/group (chow), N=7-8/group (HFD), *p<0.01.

Supplemental Table 6. List of qPCR primers used in this study.

Supplemental Figures

Supplemental Figure 1

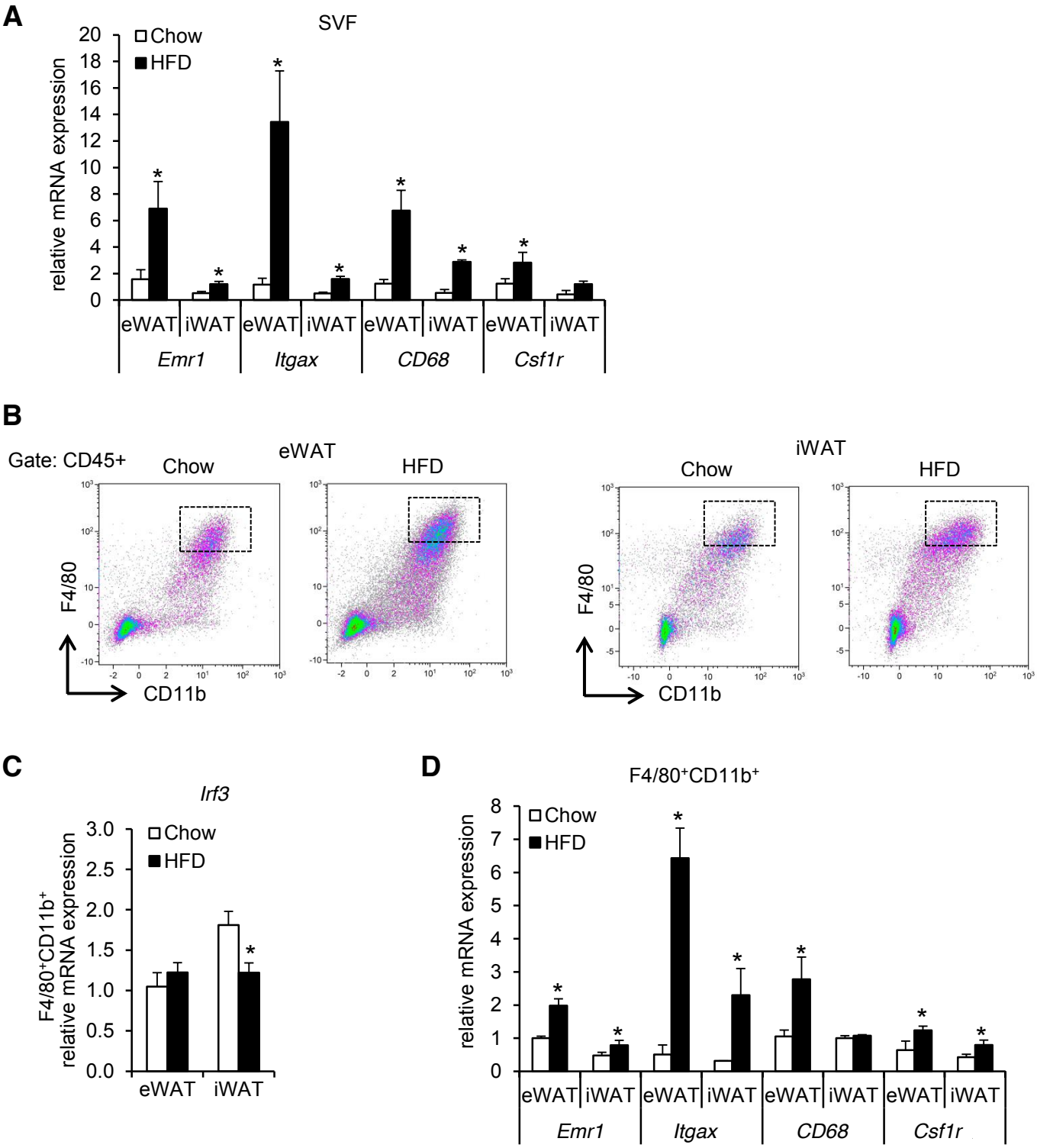

Supplemental Figure 1. Expression of macrophage markers in SVF from HFD mice.
(**A**) Expression of macrophage marker genes in isolated stromal-vascular fraction (SVF) of adipose tissue (eWAT and iWAT) from chow and HFD fed mice by qPCR. (**B**) SVF isolated from eWAT and iWAT of chow and HFD fed mice were gated for live CD45$^+$ cells. Representative scatter-plot showing macrophages stained with F4/80 and CD11b antibody. (**C** and **D**) Expression of *Irf3* and macrophage marker genes in sorted F4/80$^+$ CD11b$^+$ macrophages by FACS. n=5-6/group. Data is presented as mean ± SEM. For all data, **p*<0.05.

Supplemental Figure 2

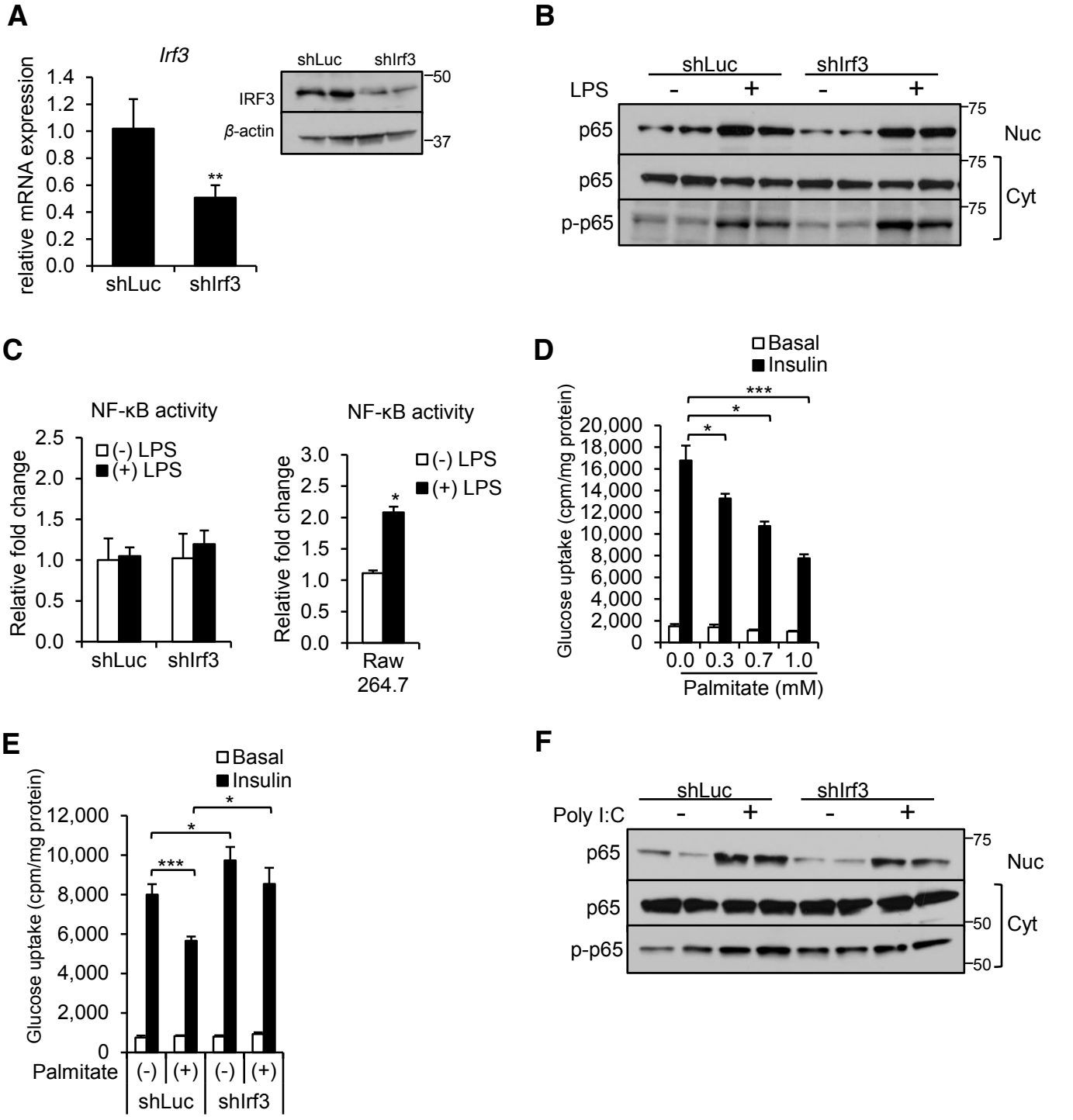

Supplemental Figure 2. Effect of LPS, palmitate and poly I:C treatment in the absence or presence of IRF3. (**A**) Expression of mouse IRF3 at mRNA and protein level in mature 3T3-L1 adipocytes transduced with lentivirus expressing shRNA against mouse Irf3, determined by qPCR and Western blotting. n=4. (**B**) Western blot showing effect of LPS treatment on protein levels of p65 and phospho-p65 in isolated nuclei and/or cytosolic fraction of 3T3-L1 adipocytes. (**C**) Effect of LPS (700 ng/ml) treatment for 6 days on NF-κB activity in the isolated nuclei fraction from 3T3-L1 adipocytes using TransAm NF-κB activity kit. Lysate from Raw 264.7 cells treated with LPS (700 ng/ml) for 1 h was used as a positive control. (**D**) Basal and insulin-stimulated glucose uptake in 3T3-L1 adipocytes after treatment with varying doses of palmitate for 48 h. (**E**) Basal and insulin-stimulated glucose uptake in 3T3-L1 adipocytes transduced with lentivirus expressing shRNA against Irf3 or shLuc control hairpin in the absence or presence of palmitate treatment (1 mM). (**F**) Western blot showing effect of poly I:C treatment on protein levels of p65 and phospho-p65 in isolated nuclei and/or cytosolic fraction of 3T3-L1 adipocytes. Data is presented as mean ± SEM. ***p<0.001, **p<0.01, *p<0.05.

Supplemental Figure 3

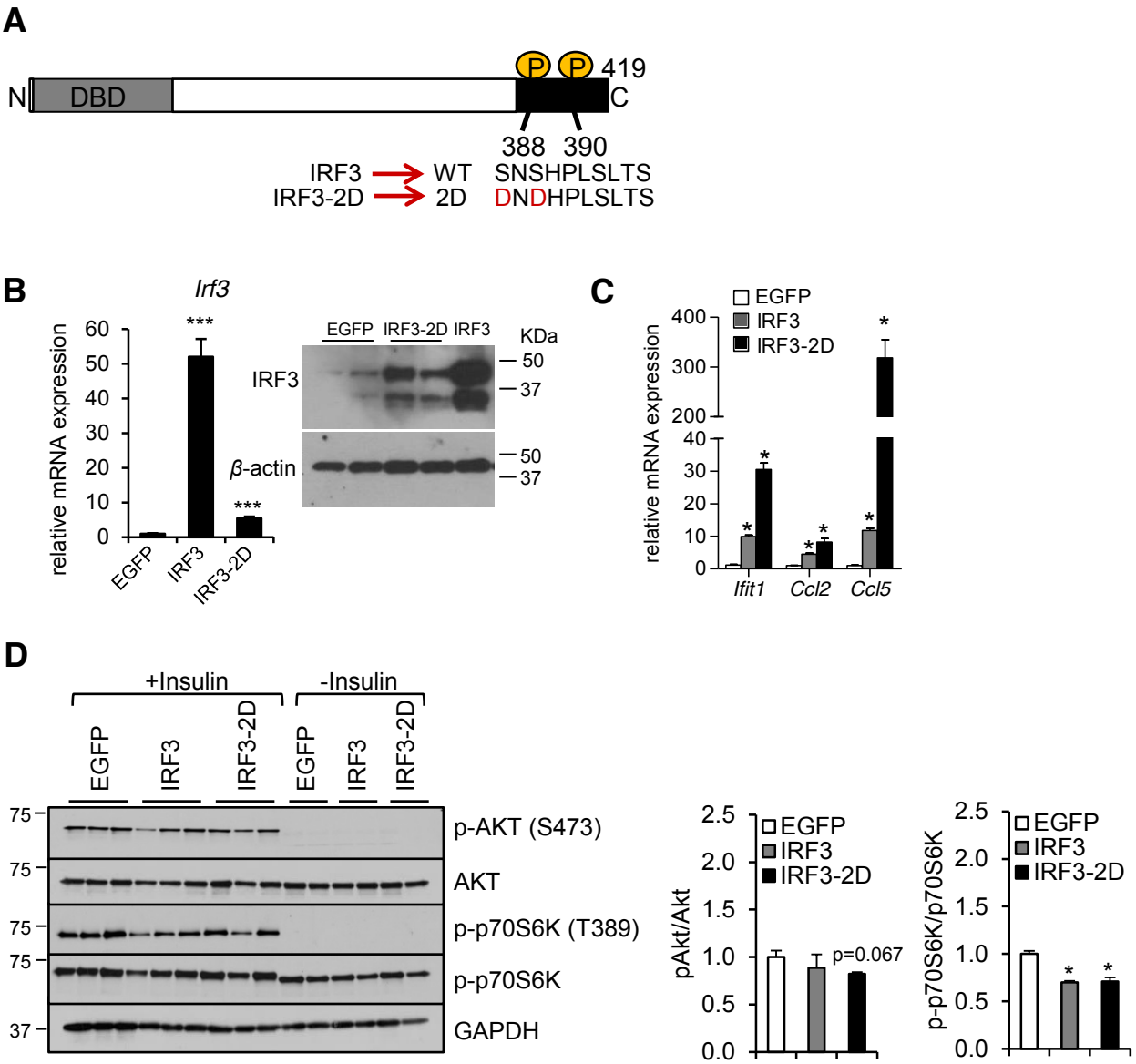

Supplemental Figure 3. Effect of IRF3 overexpression on insulin signaling in 3T3-L1 adipocytes.
(**A**) Schematic representation of the wild-type IRF3 and mutant IRF3 (IRF3-2D) protein. (**B**) Overexpression of mouse IRF3 and IRF3-2D mutant at mRNA and protein level in mature 3T3-L1 adipocytes transduced with lentivirus, determined by qPCR and Western blotting. n=4. (**C**) Effect of IRF3 overexpression on inflammatory gene expression by lentivirus transduction in mature 3T3-L1 adipocytes using qPCR. n=4. (**D**) Effect of IRF3 overexpression on insulin signaling in mature 3T3-L1 adipocytes by Western blotting. Data is presented as mean ± SEM. *p<0.05, ***p<0.001.

Supplemental Figure 4

A

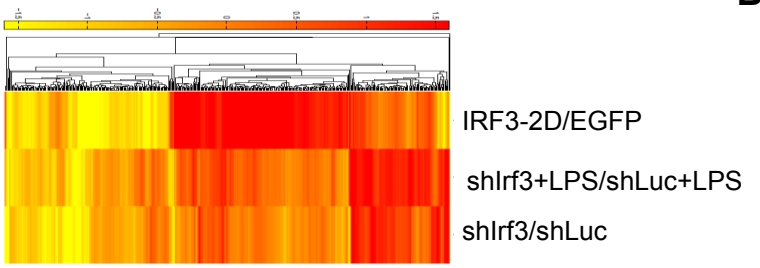

B

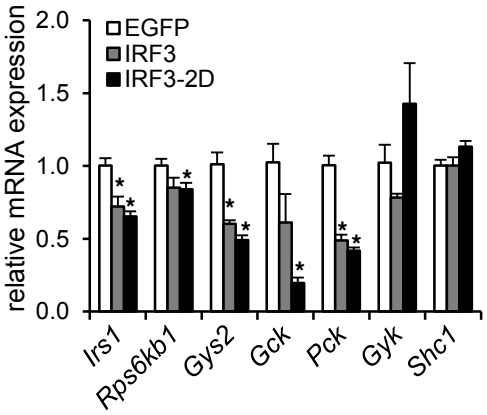

C

UP/UP	IRF3-2D vs EGFP	shIrf3 vs shLuc	shLuc vs shLuc+LPS	shIrf3 vs shIrf3+LPS	shIrf3+LPS vs shLuc+LPS
IRF3-2D vs EGFP	557	50	61	103	86
shIrf3 vs shLuc		271	30	22	174
shLuc vs shLuc+LPS			429	281	25
shIrf3 vs shIrf3+LPS				610	51
shIrf3+LPS vs shLuc+LPS					457

D

DOWN/DOWN	IRF3-2D vs EGFP	shIrf3 vs shLuc	shLuc vs shLuc+LPS	shIrf3 vs shIrf3+LPS	shIrf3+LPS vs shLuc+LPS
IRF3-2D vs EGFP	505	136	44	34	104
shIrf3 vs shLuc		376	36	9	142
shLuc vs shLuc+LPS			419	207	8
shIrf3 vs shIrf3+LPS				284	8
shLuc+LPS vs shIrf3+LPS					221

E

UP/DOWN	shIrf3 vs shLuc	shLuc vs shLuc+LPS	shIrf3 vs shIrf3+LPS	shIrf3+LPS vs shLuc+LPS
IRF3-2D vs EGFP	36	40	19	11
shIrf3 vs shLuc		66	68	0
shLuc vs shLuc+LPS			0	154
shIrf3 vs shIrf3+LPS				74

F

DOWN/UP	shIrf3 vs shLuc	shLuc vs shLuc+LPS	shIrf3 vs shIrf3+LPS	shIrf3+LPS vs shLuc+LPS
IRF3-2D vs EGFP	12	76	90	17
shIrf3 vs shLuc		50	116	0
shLuc vs shLuc+LPS			1	72
shIrf3 vs shIrf3+LPS				67

Supplemental Figure 4. Differentially regulated genes by IRF3 overexpression or knockdown in the absence or presence of LPS.

(**A**) Heat map showing gene expression fold change between three groups (IRF3-2D vs EGFP, shIrf3 vs shLuc, and shIrf3 vs shLuc in the presence of LPS). Scale is log2 fold change. (**B**) Effect of IRF3 overexpression in mature 3T3-L1 adipocytes on insulin signaling genes from Cluster 2 of RNA-seq, validated by qPCR. Data is presented as mean ± SEM. *p<0.05. (**C-F**) Number of upregulated or downregulated genes by IRF3 expression between five groups (IRF3-2D vs EGFP, shIrf3 vs shLuc, shLuc vs shLuc in the presence of LPS, shIrf3 vs shIrf3 in the presence of LPS, and shIrf3 vs shLuc in the presence of LPS).

Supplemental Figure 5

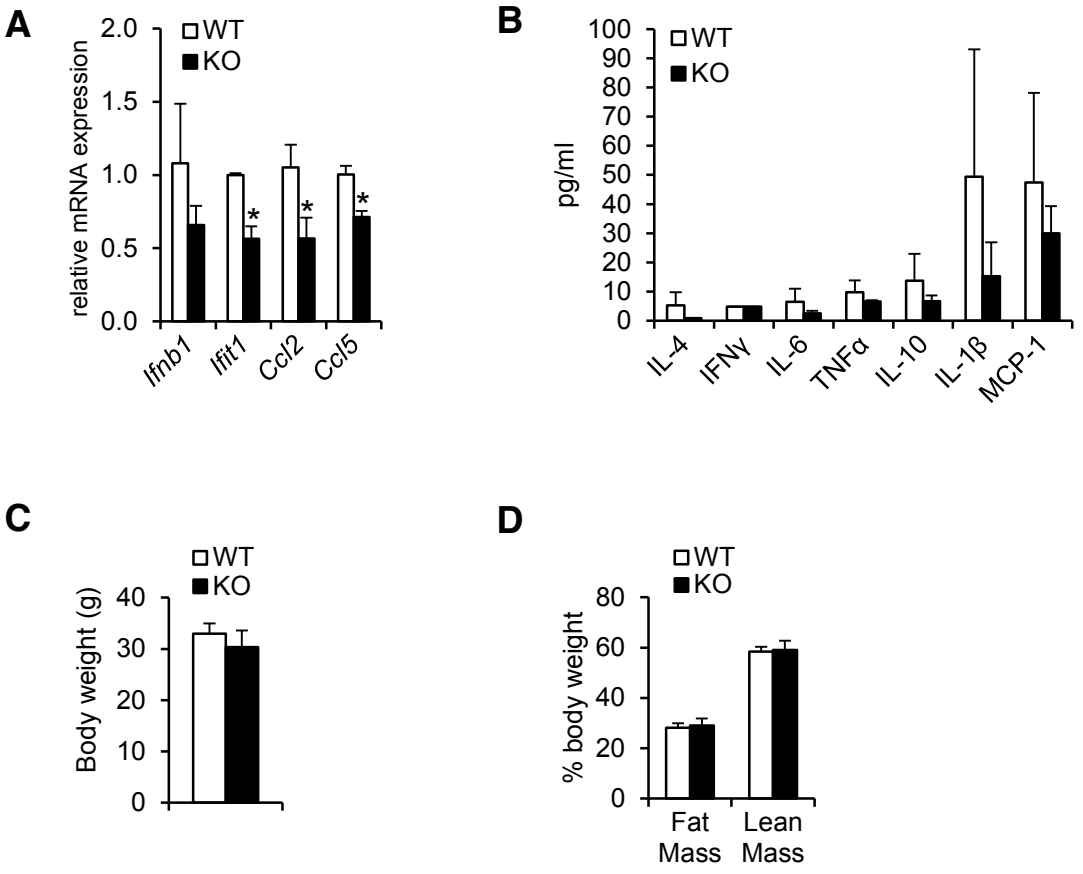

Supplemental Figure 5. Characteristics of *Irf3*$^{-/-}$ mice on chow diet.
(**A**) Expression of IRF3 target inflammatory genes in eWAT by qPCR. (**B**) Plasma cytokine levels measured in *Irf3*$^{-/-}$ mice. (**C**) Body weight of WT and *Irf3*$^{-/-}$ mice. (**D**) Body composition determined in *Irf3*$^{-/-}$ mice. All data from male chow-fed 16 week old control and *Irf3*$^{-/-}$ mice, n=6-7/genotype. Data is presented as mean ± SEM. For all data, **p*<0.05.

Supplemental Figure 6

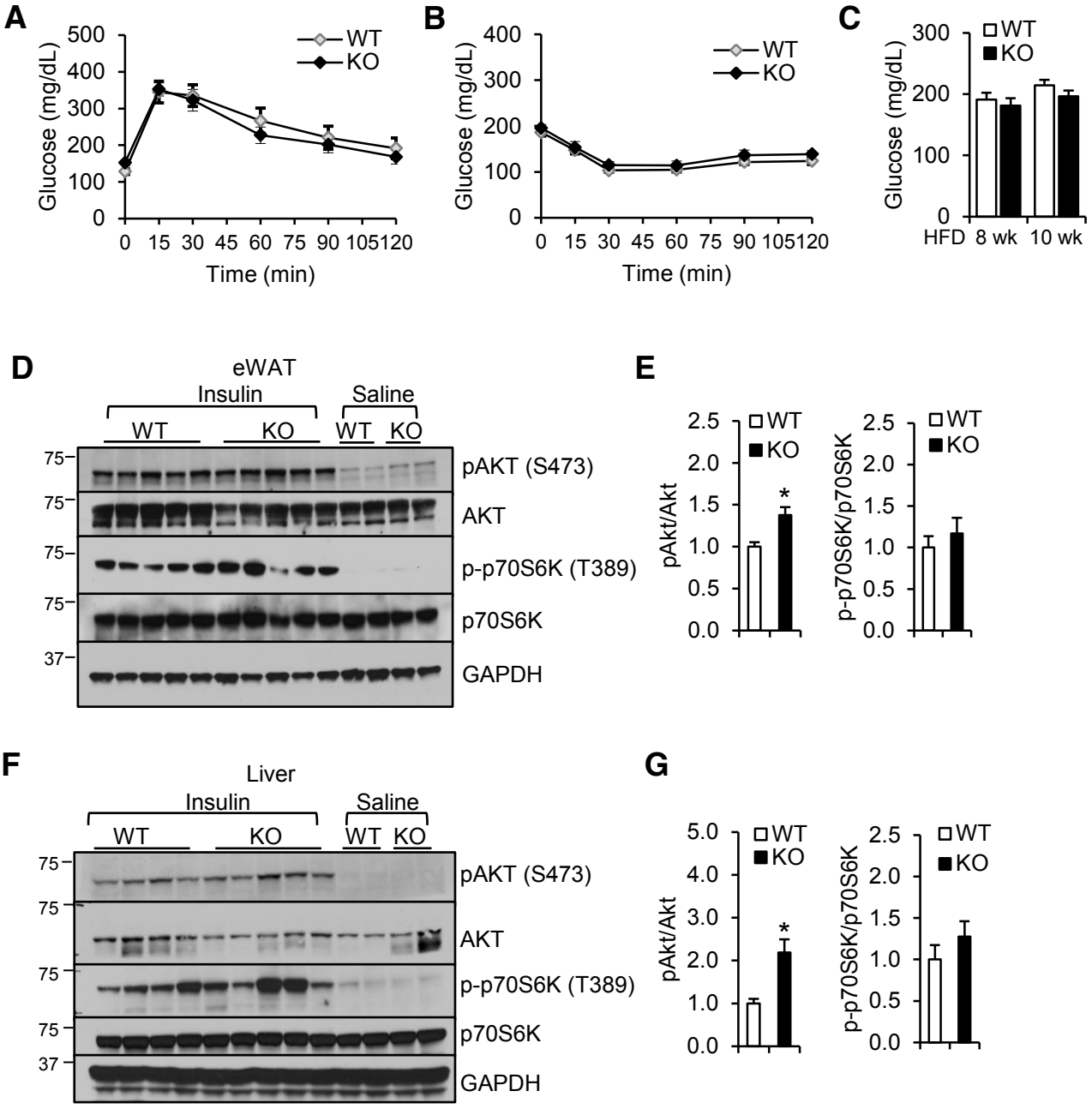

Supplemental Figure 6. Effect of Irf3 deficiency on insulin sensitivity in chow and HFD fed mice.
(**A**) Glucose tolerance test (GTT) in *Irf3*$^{-/-}$ mice after 8 weeks on chow diet. (**B**) Insulin tolerance test (ITT) in *Irf3*$^{-/-}$ mice after 10 weeks on chow diet. (**C**) Fasting plasma glucose levels in *Irf3*$^{-/-}$ mice after 8 and 10 weeks on HFD. (**D**) Western blot showing insulin signaling in eWAT of *Irf3*$^{-/-}$ mice on HFD. (**E**) Quantification of Western blot in Supplemental Figure 6D. (**F**) Western blot showing insulin signaling in liver of *Irf3*$^{-/-}$ mice on HFD. (**G**) Quantification of Western blot in Supplemental Figure 6F. N=6-7/genotype for chow studies. N= 7-8/genotype for HFD studies. Data is presented as mean ± SEM. For all data *p<0.05.

Supplemental Figure 7

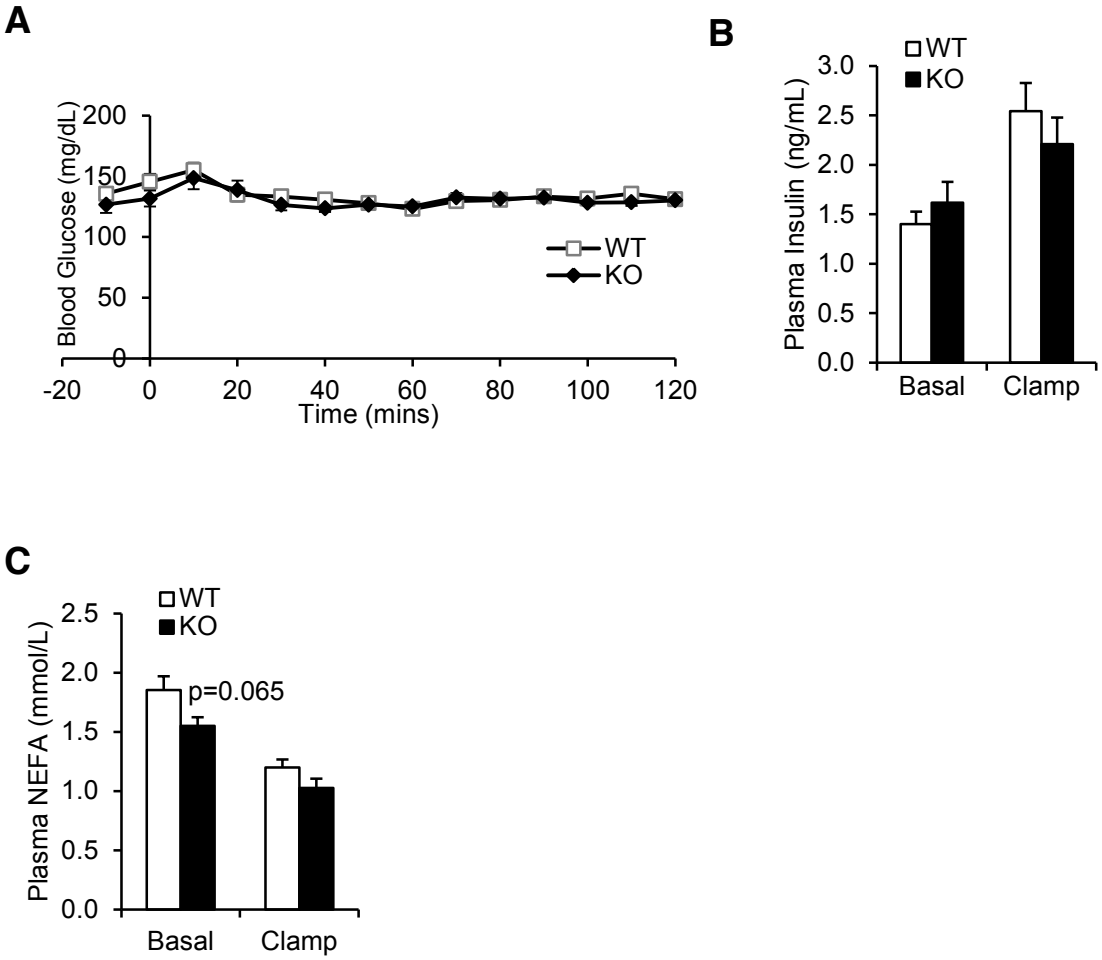

Supplemental Figure 7. Hyperinsulinemic-euglycemic clamp in *Irf3*$^{-/-}$ mice on HFD.
(**A**) Fasting and clamped glucose levels in control and *Irf3*$^{-/-}$ mice after 8 weeks of HFD feeding. (**B**) Fasting and clamped insulin levels in control and *Irf3*$^{-/-}$ mice. (**C**) Fasting and clamped non-esterified fatty acids (NEFAs) levels in control and *Irf3*$^{-/-}$ mice. For all data N=8-10 per genotype. Data is presented as mean ± SEM.

Supplemental Figure 8

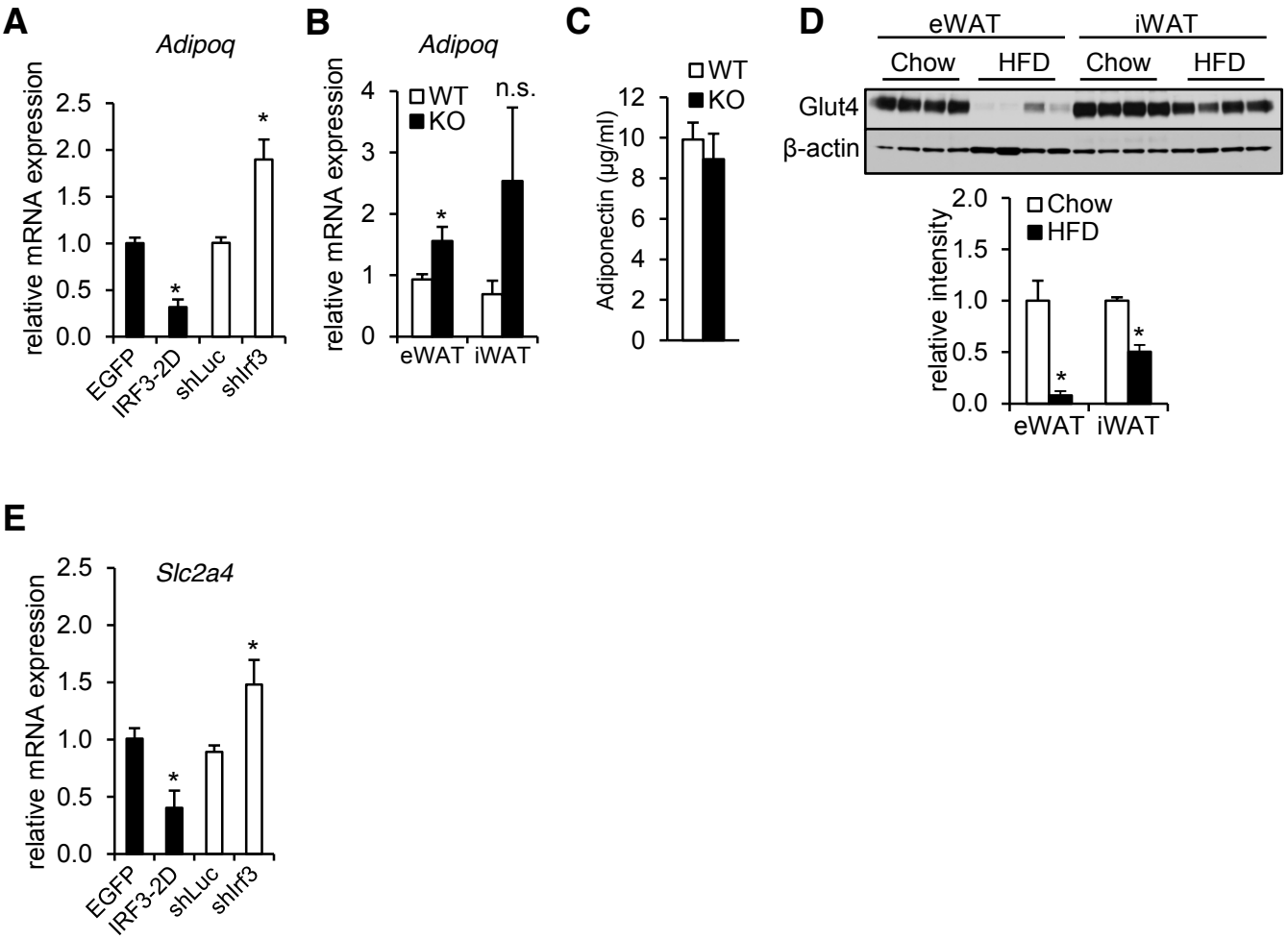

Supplemental Figure 8. Effect of Irf3 deficiency on Glut4 and adiponectin levels in HFD fed mice.
(**A**) Adiponectin (*Adipoq*) mRNA levels in 3T3-L1 adipocytes following overexpression or knockdown of IRF3 by qPCR. (**B**) Expression of *Adipoq* in eWAT and iWAT of WT and *Irf3*$^{-/-}$ mice on HFD by qPCR. (**C**) Plasma adiponectin levels in WT and *Irf3*$^{-/-}$ mice on HFD. (**D**) Glut4 protein levels in eWAT and iWAT of chow vs HFD mice determined by Western blotting. (**E**) Gene expression of *Slc2a4* in 3T3-L1 adipocytes with overexpression and knockdown of murine IRF3. N=4 for in vitro studies. N= 7-8/genotype for HFD studies. Data is presented as mean ± SEM. For all data *p<0.05.

Supplemental Figure 9

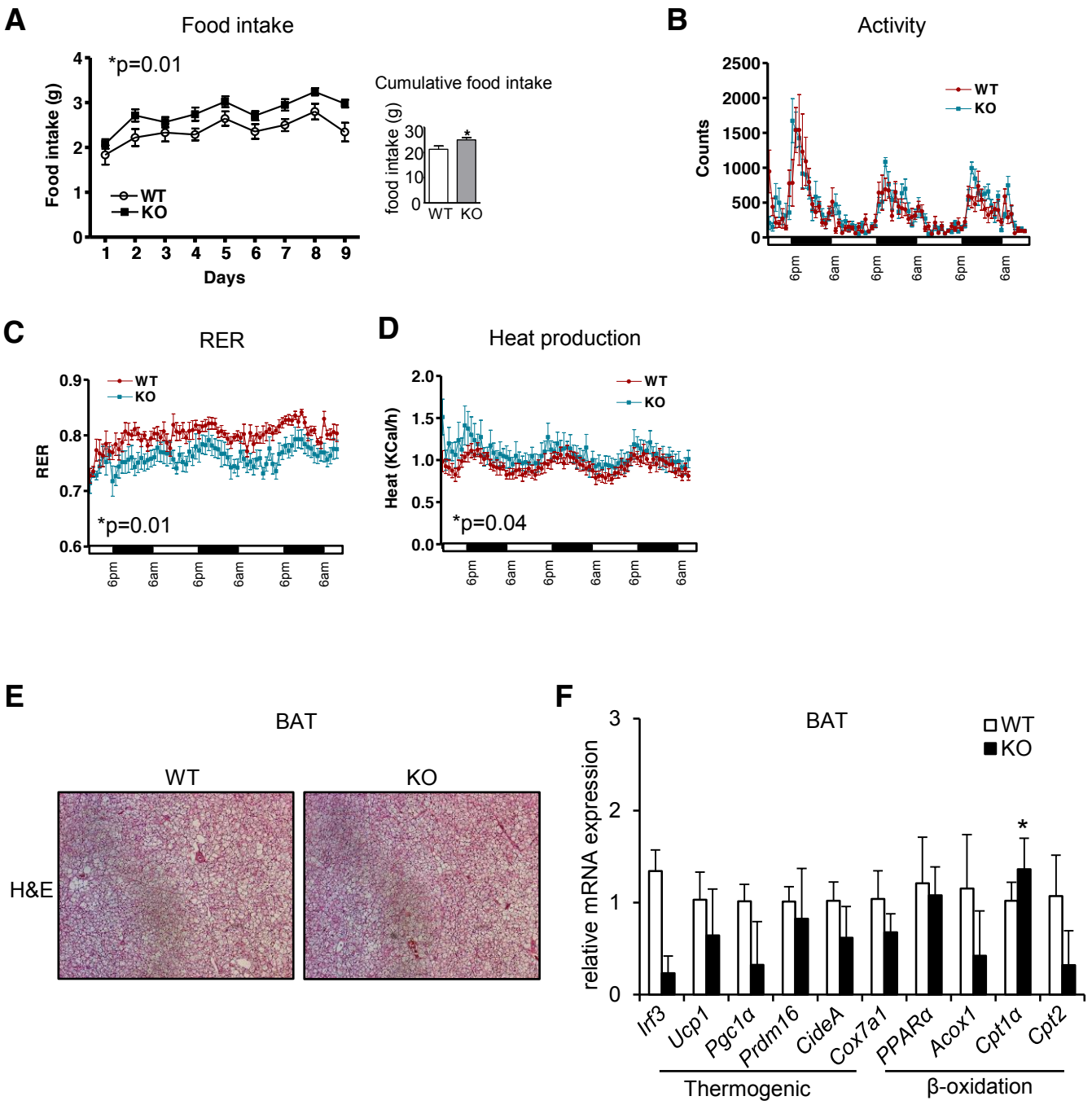

Supplemental Figure 9. Energy expenditure and expression of thermogenic genes in BAT of *Irf3*$^{-/-}$ mice on HFD.

CLAMS study was performed on *Irf3*$^{-/-}$ mice upon 16 weeks of HFD feeding to determine effect on (**A**) food intake, (**B**) activity, (**C**) respiratory exchange ratio (RER), and (**D**) heat production. (**E**) Histology showing H&E staining in BAT of *Irf3*$^{-/-}$ mice on HFD (10X magnification). (**F**) Expression of thermogenic and β-oxidation genes in BAT of *Irf3*$^{-/-}$ mice on HFD. For all data n=7-8/genotype. Data is presented as mean ± SEM. For all data, **p*<0.05.

Supplemental Figure 10

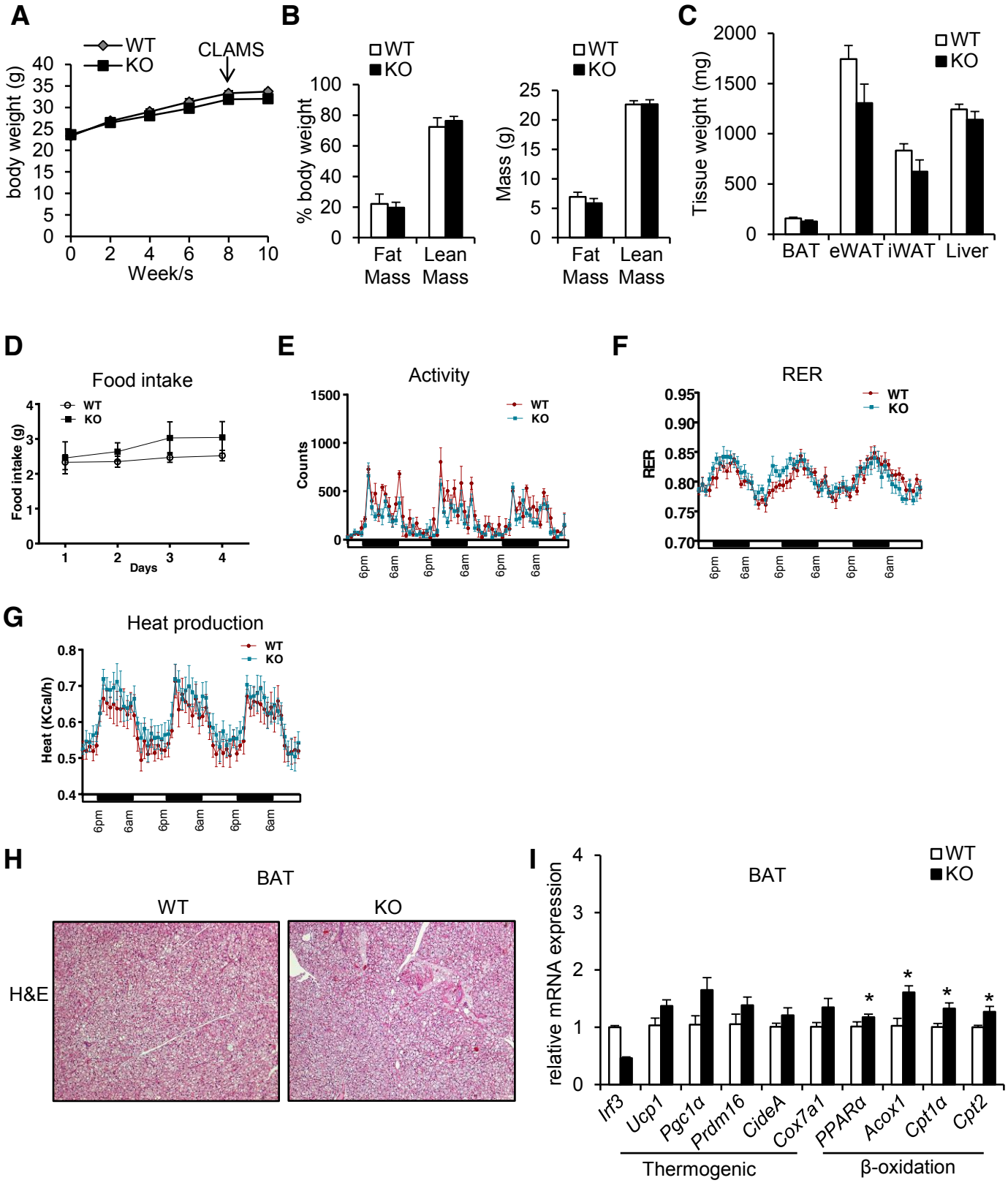

Supplemental Figure 10. Energy expenditure and expression of thermogenic genes in BAT of *Irf3*$^{-/-}$ mice on HFD before body weight divergence.

Male wild-type and *Irf3*$^{-/-}$ mice were fed HFD and used for CLAMS study. N=6/genotype. (**A**) Body weight of WT and *Irf3*$^{-/-}$ mice during 10 weeks HFD feeding. (**B**) Body composition of WT and *Irf3*$^{-/-}$ mice at 8 weeks of HFD feeding. (**C**) Tissue weight of WT and *Irf3*$^{-/-}$ mice after 10 weeks on HFD. (**D**) Food intake, (**E**) activity, (**F**) respiratory exchange ratio (RER), and (**G**) heat production in *Irf3*$^{-/-}$ mice upon 8 weeks of HFD. (**H**) Histology showing H&E staining in BAT of *Irf3*$^{-/-}$ mice upon 10 weeks of HFD (10X magnification). (**I**) Expression of thermogenic and β-oxidation genes in BAT of *Irf3*$^{-/-}$ mice upon 10 weeks of HFD. Data is presented as mean ± SEM. For all data *p<0.05.

Supplemental Table 1. Human subjects characteristic and plasma parameters.

Parameters	Non-Diabetic (Mean±SD)	Diabetic (Mean±SD)
Number (N)	48	45
Gender(Female/Male)	25/23	21/24
Age (yrs)	44.79±11.82	53.98±7.83
BMI (kg/m^2)	30.88±4.72	31.50±3.50
Fasting Blood Glucose (mmol/l)	5.40±1.11	8.57±2.66
HDL cholesterol (mmol/l)	1.30±0.35	1.16±0.32
LDL cholesterol (mmol/l)	3.31±0.83	2.82±1.16
Triglycerides (mmol/l)	1.09±0.67	1.67±1.02
Cholesterol (mmol/l)	5.11±0.96	4.85±1.36
HbA1C (%)	5.83±1.09	7.94±1.50

Supplemental Table 2. List of genes coordinately regulated by overexpression and knock-down of murine IRF3. Numbers represent log2 fold change with ≤25% FDR.

Gene	IRF3-2D vs EGFP	shIrf3 vs shLuc
Adam6a	-1.5	1.9
Mmp9	-1.3	1.3
Gldc	-1.1	0.8
Lyl1	-0.9	0.7
Mmp8	-0.9	2.2
Mmp13	-0.9	1.5
Srpx2	-0.9	0.5
Otop1	-0.7	0.7
Nwd1	-0.7	1.7
Pygb	-0.6	0.5
Ces1a	-0.6	0.7
Pappa2	-0.6	0.5
Atp1b1	-0.5	0.6
Thbs1	-0.5	0.4
DQ539915	-0.4	0.5
Fbxl13	-0.4	0.6
Gpx1	-0.4	0.4
Dcn	-0.3	0.4
Npr3	-0.3	0.4
Plat	-0.3	0.8
Pros1	-0.3	0.5
Tmeff1	-0.3	0.3
Usp35	-0.3	0.4
Irf3	0.2	-0.7
Atp10d	0.3	-0.3
Itih4	0.3	-1
Laptm4b	0.3	-0.5
Ces4a	0.4	-0.7
Emp1	0.4	-0.5
Tsta3	0.4	-0.3
C4b	0.5	-1.6
H2-Q8	0.5	-0.6
AW112010	0.5	-0.9
Tmsb4x	0.6	-0.6
Tdo2	0.6	-0.8
Bub1	0.6	-0.7
Pde4b	0.6	-0.6
Exo1	0.6	-0.7
Ifi27l2a	0.6	-0.6
Agpat9	0.7	-0.6
H2-Q1	0.7	-0.7
Cox6a2	0.7	-0.6
2410017I17Rik	0.7	-0.6
Aurkb	0.8	-0.6
Dapk1	0.8	-1.2
Gm8909	0.8	-0.5
H2-Q2	0.8	-0.7
H2-K2	0.8	-0.6
H2-K1	0.8	-0.8
H2-Bl	0.9	-0.8
Nlrc5	0.9	-0.5
Hist1h3h	1	-0.8
Cyp2b10	1	-1
H2-D1	1	-0.4
H2-Gs10	1	-0.7
H2-Q6	1.1	-0.6
H2-T23	1.2	-0.8
Gbp11	1.2	-0.8
Oasl1	1.3	-0.7
Gbp2	1.4	-0.5
Chchd10	1.4	-0.6
Nlrp2	1.5	-1.7
AI607873	1.8	-0.5
Gbp4	1.9	-0.6
Psmb9	2.3	-0.9
BC023105	2.5	-0.8
Gm12185	2.6	-0.9
Gbp10	2.8	-1.9

Supplemental Table 3. Top pathways enriched in the three major clusters identified in Figure 3B by GSEA using DAVID.

	Pathways enriched	p-value
C1	Immune response	$3.9X10^{-15}$
	Nucleotide binding	$6.8X10^{-7}$
	MHC protein complex	$4.0X10^{-5}$
C2	Insulin signaling	$3.2X10^{-2}$
C3	PPAR signaling pathway	$3.8X10^{-3}$
	Lipid transport	$1.1X10^{-2}$

Supplemental Table 4. List of pathways regulated in clusters identified in Figure 3B with ≤25% FDR.

Cluster 1 (C1)		Cluster 2 (C2)		Cluster 3 (C3)	
Pathway	**pValue**	**Pathway**	**pValue**	**Pathway**	**pValue**
immune response	3.89E-15	cell junction	0.022229	Secreted	0.00112
2'-5'-oligoadenylate synthetase 1, domain 2/C-terminal	7.34E-10	adherens junction	0.024905	extracellular region part	0.002057
2-5-oligoadenylate synthetase, ubiquitin-like region	1.27E-09	Insulin signaling pathway	0.032366	zymogen	0.002373
2-5-oligoadenylate synthetase, conserved site	2.86E-09			chemotaxis	0.003315
Guanylate-binding protein, C-terminal	6.4E-09			taxis	0.003315
Guanylate-binding protein, N-terminal	6.35E-08			triglyceride-rich lipoprotein particle	0.003657
purine nucleotide binding	7.63E-08			very-low-density lipoprotein particle	0.003657
guanine nucleotide-binding protein 1	5.04E-07			PPAR signaling pathway	0.00379
nucleotide binding	6.75E-07			metal ion-binding site:Zinc 2; in inhibited form	0.004388
purine ribonucleotide binding	6.89E-07			integrin-mediated signaling pathway	0.005257
ribonucleotide binding	6.89E-07			extracellular region	0.005369
response to virus	4.39E-06			endopeptidase activity	0.006371
2'-5'-oligoadenylate synthetase activity	1.59E-05			locomotory behavior	0.006578
nucleotidyltransferase activity	2.58E-05			coenzyme A	0.008045
adenyl nucleotide binding	2.6E-05			metal ion-binding site:Zinc 2; catalytic	0.00864
purine nucleoside binding	3.07E-05			C-acyltransferase activity	0.009664
nucleoside binding	3.48E-05			Peptidase M10A, matrix metallopeotidase	0.010561
MHC protein complex	4.03E-05			lipid transport	0.011292
HIN-200/IF120x	5.58E-05			Peptidoglycan binding-like	0.012967
class I histocompatibility antigen	6.83E-05			extracellular matrix	0.01362
mhc i	8.77E-05			Peptidase_M10A_matrix	0.013828
antigen processing and presentation	0.000113			Acyltransferase	0.013915
ATP binding	0.000142			Nitrogen metabolism	0.014892
Nucleotidyltransferase	0.000143			Hemopexin/matrixin	0.015587
adenyl ribonucleotide binding	0.000173			serpin	0.0161
				Hemopexin/matrixin, repeat	0.016975
				Hemopexin/matrixin, conserved site	0.016975
				integrin	0.018269
				domain:Hemopexin-like 4	0.019033
				metal ion-binding site:Calcium 3; via carbonyl oxygen	0.019033
				domain:Hemopexin-like 3	0.019033
				cofactor binding	0.01993
				Biosynthesis of unsaturated fatty acids	0.020237
				proteinaceous extracellular matrix	0.020591

Supplemental Table 5. Plasma parameters of *Irf3*$^{-/-}$ mice on chow and high-fat diet. Plasma samples were collected from 16 week old male *Irf3*$^{-/-}$ mice on chow and high-fat diet (HFD) in the fed state. Data is represented as mean ± SEM. N=6-7/group (chow), N=7-8/group (HFD), **p*<0.01.

Plasma Parameter	Chow		HFD	
	WT	*Irf3*$^{-/-}$	WT	*Irf3*$^{-/-}$
Glucose (mg/dl)	224.0 ± 13.5	197.1 ± 7.4	211.6 ± 9.5	218.1 ± 22.3
Insulin (ng/ml)	1.0 ± 0.4	0.6 ± 0.1	4.2 ± 1.1	1.5 ± 0.4*
TG (mg/dl)	60.4 ± 5.1	55.2 ± 3.6	83.3 ± 4.8	90.9 ± 7.4
NEFA (mM)	0.4 ± 0.06	0.3 ± 0.08	0.8 ± 0.03	0.8 ± 0.09

Supplemental Table 6. List of qPCR primers used in this study.

Gene Name (Symbol)	Primer sequence (5' – 3')	GenBank Acc. No.
2'-5' oligoadenylate synthetase-like 2 (Oasl2)	F: TTGTGCGGAGGATCAGGTACT R: TGATGGTGTCGCAGTCTTTGA	NM_011854
Acyl-Coenzyme A oxidase 1, palmitoyl (Acox1)	F: TCCAGACTTCCAACATGAGGA R: CTGGGCGTAGGTGCCAATTA	NM_015729
Adhesion G protein-coupled receptor E1 (Adgre1 or F4/80)	F: CTTTGGCTATGGGCTTCCAGTC R: GCAAGGAGGACAGAGTTTATCGTG	NM_010130
Adiponectin (Adipoq)	F: CAGTGGATCTGACGACACCAA R: CTGGGCAGGATTAAGAGGAACA	NM_009605
Carnitine palmitoyltransferase 2 (Cpt2)	F: CAGCACAGCATCGTACCCA R: TCCCAATGCCGTTCTCAAAAT	NM_009949
Carnitine palmitoyltransferase 1a (Cpt1a)	F: CACCAACGGGCTCATCTTCTA R: CAAAATGACCTAGCCTTCTATCGAA	NM_013495
CD68 antigen (Cd68)	F: CTTCCCACAGGCAGCACAG R: AATGATGAGAGGCAGCAAGAGG	NM_001291058
Cell death-inducing DNA fragmentation factor, alpha subunit-like effector A (Cidea)	F: TACTACCCGGTGTCCATTTCT R: ATCACAACTGGCCTGGTTACG	NM_007702
Chemokine (C-C motif) ligand 2 (Ccl2)	F: TTAAAAACCTGGATCGGAACCAA R: GCATTAGCTTCAGATTTACGGGT	NM_011333
Chemokine (C-C motif) ligand 5 (Ccl5)	F: GCTGCTTTGCCTACCTCTCC R: TCGAGTGACAAACACGACTGC	NM_013653
Chemokine (C-C motif) ligand 6 (Ccl6)	F: GGCTGGCCTCATACAAGAAATG R: TGTGGCATAAGAGAAGCAGCA	NM_009139
Colony stimulating factor 1 receptor (Csf1r)	F:GCATACAGCATTACAACTGGACCTACC R: CAGGACATCAGAGCCATTCACAG	NM_001037859
Cytochrome c oxidase subunit VIIa 1 (Cox7a1)	F: ATGAGGGCCCTACGGGTCTC R: CATTGTCGGCCTGGAAGAG	NM_009944
Glucokinase (Gck)	F: GAGATGGATGTGGTGGCAAT R: ACCAGCTCCACATTCTGCAT	NM_010292
Glycerol kinase (Gyk)	F: AGGATGGACAGGCCAAAAA R: GCCCGTGTTGCACAATAAGA	NM_008194
Glucose transporter type 4 (Slc2a4)	F: TCATTGTCGGCATGGGTTT R: CGGCAAATAGAAGGAAGACGTA	NM_009204
Glycogen synthase 2 (Gys2)	F: CCAGCTTGACAAGTTCGACA R: ATCAGGCTTCCTCTTCAGCA	NM_145572
Insulin receptor substrate 1 (Irs1)	F: CTGGAGTATTATGAGAACGAGAAGAAGTGG R: GTAGAGAGCCACCAGGTGCTTGT	NM_010570
Integrin alpha X (Itgax)	F: CTGGATAGCCTTTCTTCTGCTG R: GCACACTGTGTCCGAACTCA	NM_021334
Interferon alpha 1 (Ifnα1)	F: GGACTTTGGATTCCCGCAGGAGAAG R: GCTGCATCAGACAGCCTTGCAGGTC	NM_010502
Interferon beta 1 (Ifnβ1)	F: CAGCTCCAAGAAAGGACGAAC R: GGCAGTGTAACTCTTCTGCAT	NM_010510
Interferon-induced protein with tetratricopeptide repeats 1 (Ifit1)	F: CAAGGCAGGTTTCTGAGGAG R: TGAAGCAGATTCTCCATGACC	NM_008331
Interferon-induced protein with tetratricopeptide repeats 2 (Ifit2)	F: TCTGATTCTGAGGCCTTGCA R: CTTGCTGACCTCCTCCATTCTC	NM_008332
Interferon-induced protein with tetratricopeptide repeats 3 (Ifit3)	F: CCTACATAAAGCACCTAGATGGC R: ATGTGATAGTAGATCCAGGCGT	NM_010501
Interferon Regulatory Factor 3 (Irf3)	F: GGCTTGTGATGGTCAAGGTT R: CATGTCCTCCACCAAGTCCT	NM_016849

Continued..

Supplemental Table 6.. continued

Gene Name (Symbol)	Primer sequence (5' – 3')	GenBank Acc. No.
ISG15 ubiquitin-like modifier (Isg15)	F: CATCTATGAGGTCTTTCTGACGC R: TTAGGCCATACTCCCCCAGC	NM_015783
Lipocalin 2 (Lcn2)	F: ATGCACAGGTATCCTCAGGT R: TGGCGAACTGGTTGTAGTCC	NM_008491
Nitric oxide synthase 2, inducible (Nos2)	F: CCAAGCCCTCACCTACTTCC R: CTCTGAGGGCTGACACAAGG	NM_010927
Peroxisome proliferator activated receptor alpha (Pparα)	F: GTACCACTACGGAGTTCACGCAT R: CGCCGAAAGAAGCCCTTAC	NM_011144
Peroxisome proliferative activated receptor, gamma, coactivator 1 alpha (Pgc-1α)	F: GGACATGTGCAGCCAAGACTCT R: CACTTCAATCCACCCAGAAAGCT	NM_008904
Phosphoenolpyruvate carboxykinase (Pck1)	F: CTAACTTGGCCATGATGAACC R: CTTCACTGAGGTGCCAGGAG	NM_011044
PR domain containing 16 (Prdm16)	F: TGACGGATACAGAGGTGTCAT R: ACGCTACACGGATGTACTTGA	NM_027504
Radical S-adenosyl methionine domain containing 2 (Rsad2)	F: AGCATTAGGGTGGCTAGATCC R: CTGAGTGCTGTTCCCATCTTC	NM_021384
Ribosomal protein, large, P0 (Rplp0)/36B4	F: GAGGAATCAGATGAGGATATGGGA R: AAGCAGGCTGACTTGGTTGC	NM_007475
Ribosomal protein S6 kinase polypeptide 1 (Rps6kb1)	F: GCTCTGAGGATGAGCTGGAG R: CCATGCCAAGTTCATATGGTCC	NM_001114334
Serine (or cysteine) peptidase inhibitor, clade A, member 3N (Serpina3n)	F: CAATGTCTGCGAAACTGTACC R: TTTGGGGTTGGCTATCTTGGC	NM_009252
Serine (or cysteine) peptidase inhibitor, clade A, member 3G (Serpina3g)	F: GTCACCCTGGGAAGGAACAC R: GCAGTGCAGATGCTGAATGG	NM_009251
Src homology 2 domain-containing transforming protein C1 (Shc1)	F: CCCCTCCTCCAGGACATGAA R: AGCCCATGTACCGAACCAAG	NM_001113331
Transmembrane protein 176A (Tmem176a)	F: TCCACAACCCACCCACATTG R: CACCCAGAACCACACTCAGA	NM_025326
Transmembrane protein 176B (Tmem176b)	F: CAGTCCGCTCACATCAGCAT R: TCACAAGCCCCAGCAATATC	NM_023056
Uncoupling protein 1 (mitochondrial, proton carrier) (Ucp1)	F: AGGCTTCCAGTACCATTAGGT R: CTGAGTGAGGCAAAGCTGATTT	NM_009463

Full Unedited Blots-1

Figure 1A IRF3

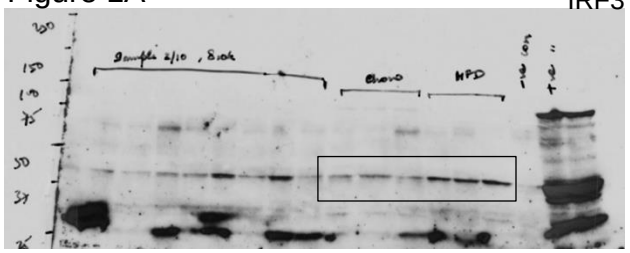

Figure 1A Caveolin-1

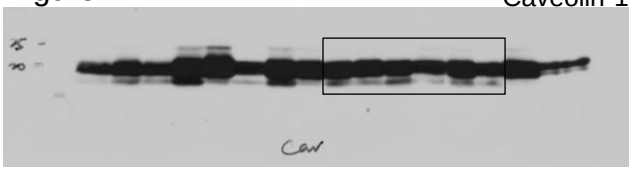

Figure 1A IRF3

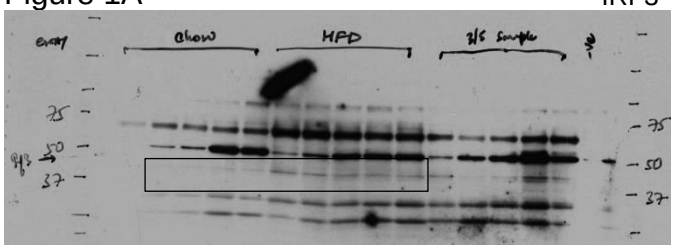

Figure 1A Caveolin-1

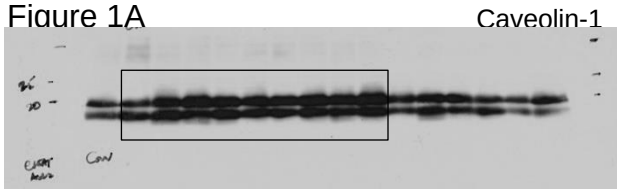

Figure 2B p-IRF3

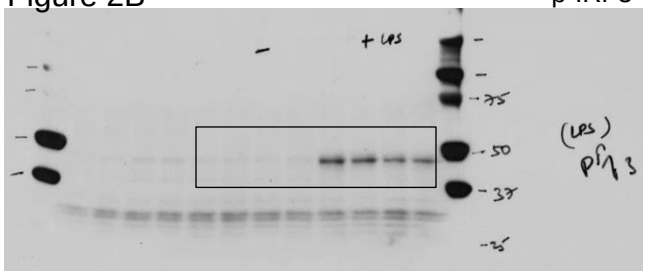

Figure 2B IRF3

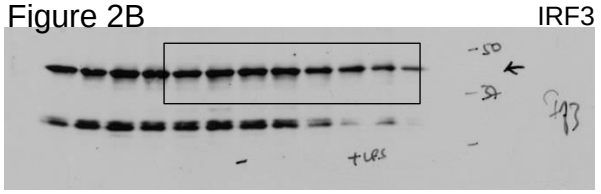

Figure 2E p-IRF3

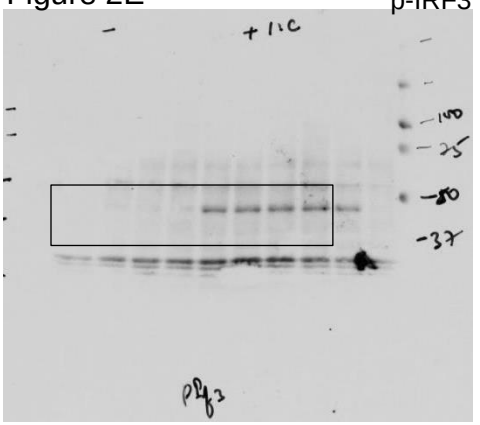

Figure 2E IRF3

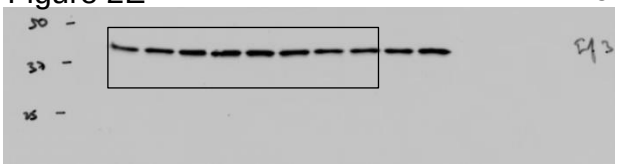

Supplemental Figure 2A

IRF3

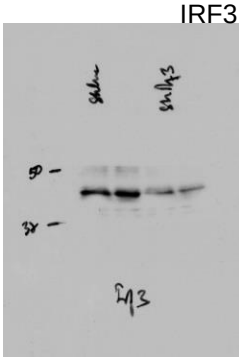

β-actin

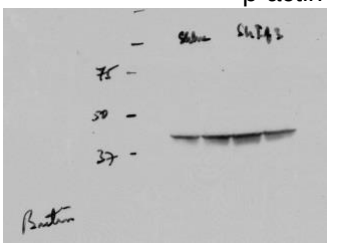

Full Unedited Blots-2

Supplemental Figure 2B p65

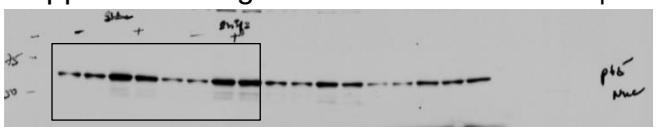

Supplemental Figure 2B p65

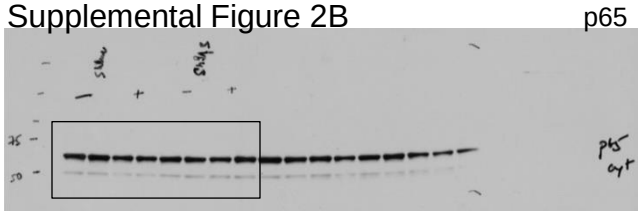

Supplemental Figure 2B p-p65

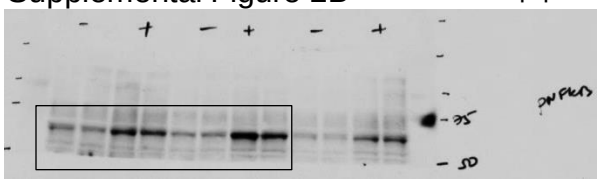

Supplemental Figure 2F p65

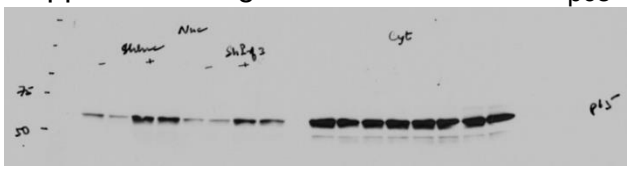

Supplemental Figure 2F p-p65

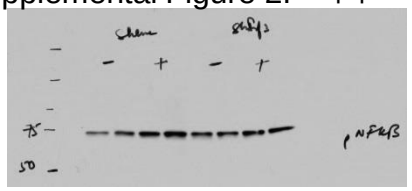

Supplemental Figure 3B IRF3

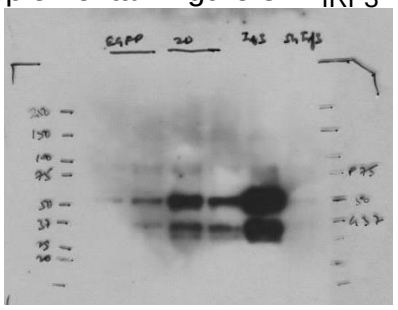

Supplemental Figure 3B β-actin

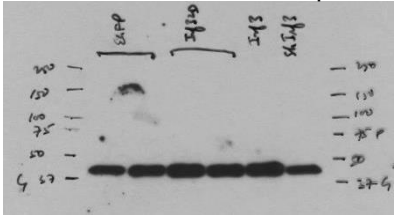

Supplemental Figure 3D p-AKT

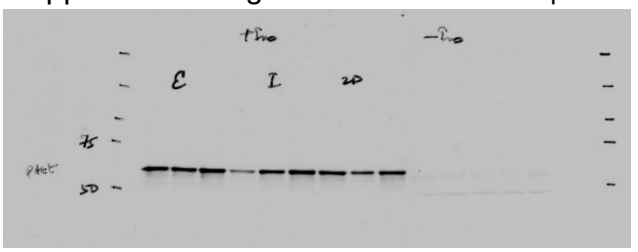

Supplemental Figure 3D AKT

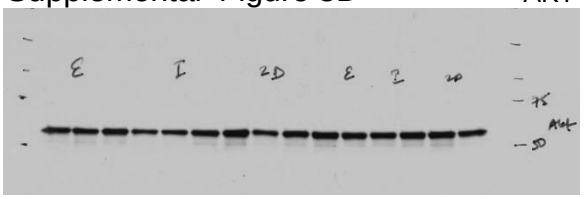

Supplemental Figure 3D p-p70S6K

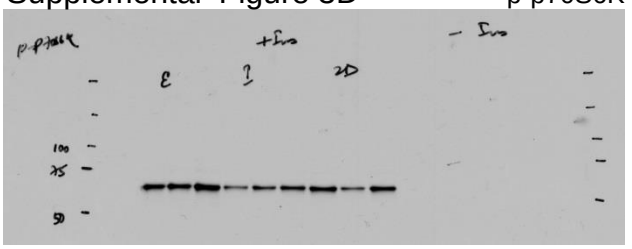

Supplemental Figure 3D p70S6K

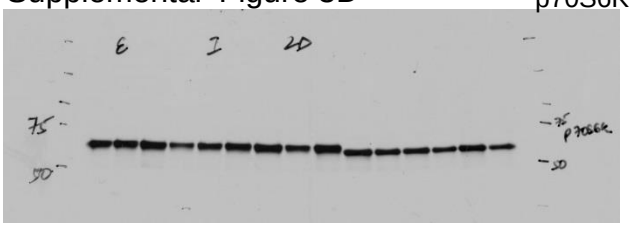

Supplemental Figure 3D GAPDH

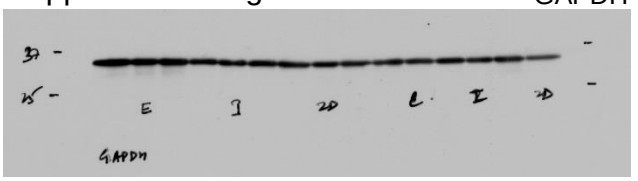

Full Unedited Blots-3

Figure 7D p-AKT

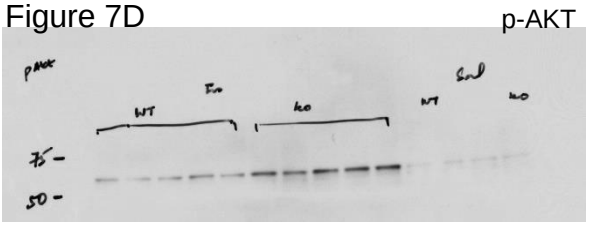

Figure 7D AKT

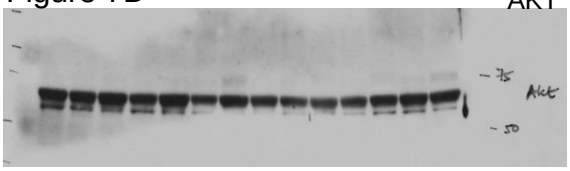

Figure 7D p-p70S6K

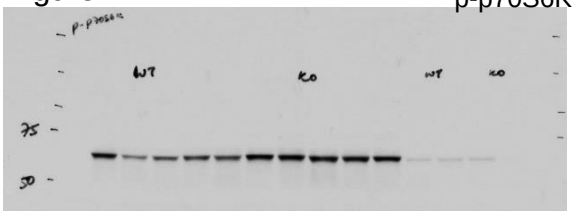

Figure 7D p70S6K

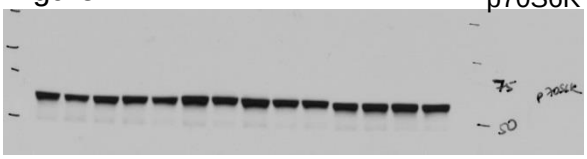

Figure 7D GAPDH

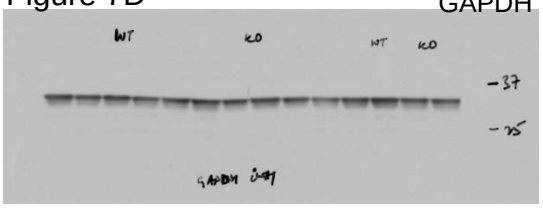

Supplemental Figure 6D p-AKT

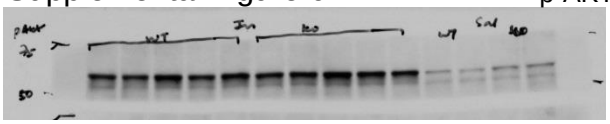

Supplemental Figure 6D AKT

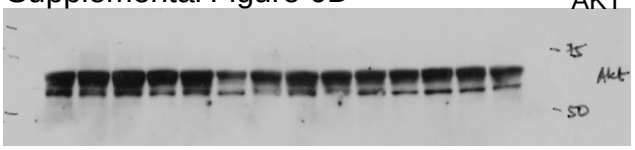

Supplemental Figure 6D p-p70S6K

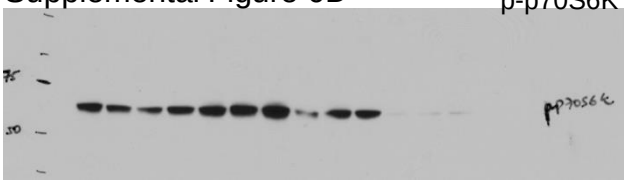

Supplemental Figure 6D p70S6K

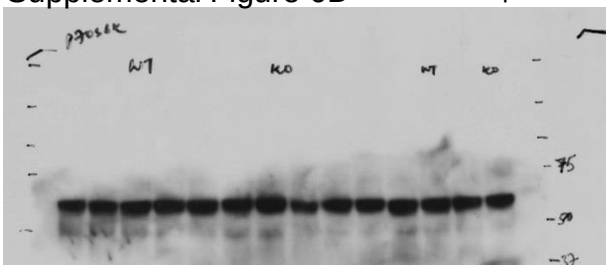

Supplemental Figure 6D GAPDH

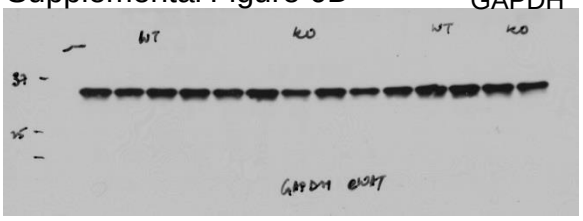

Full Unedited Blots-4

Supplemental Figure 6F p-AKT

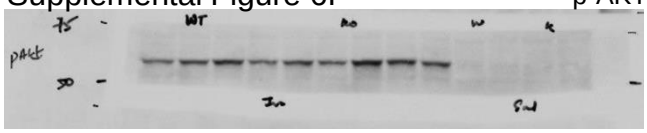

Supplemental Figure 6F AKT

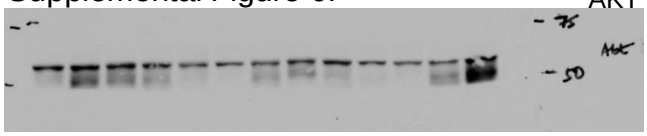

Supplemental Figure 6F p-p70S6K

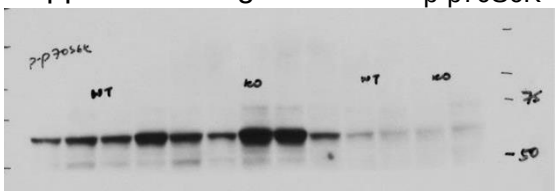

Supplemental Figure 6F p70S6K

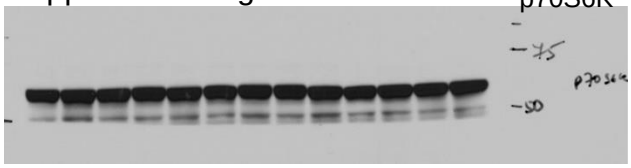

Supplemental Figure 6F GAPDH

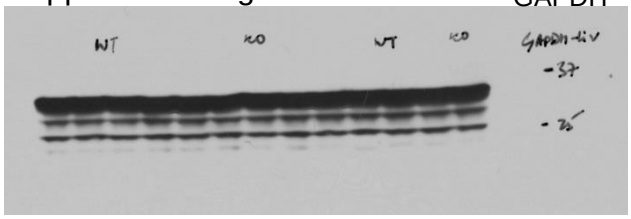

Supplemental Figure 8D Glut4

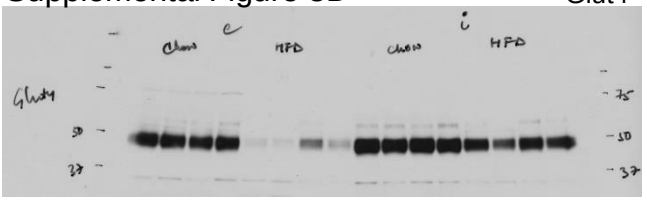

Supplemental Figure 8D β-actin

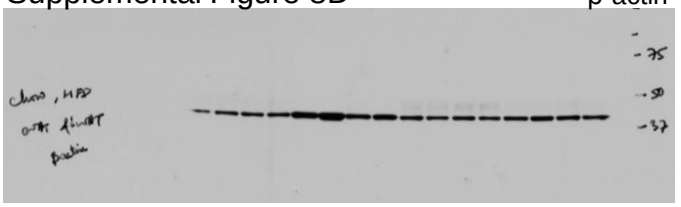

Figure 9B Glut4

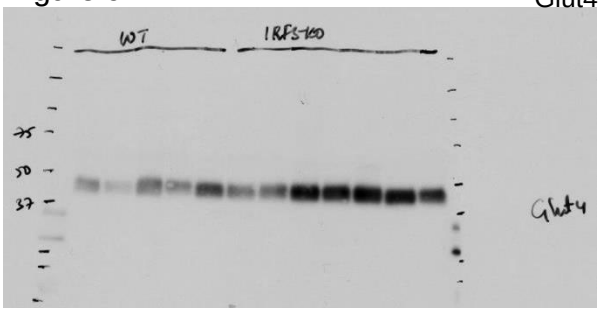

Figure 9B β-actin

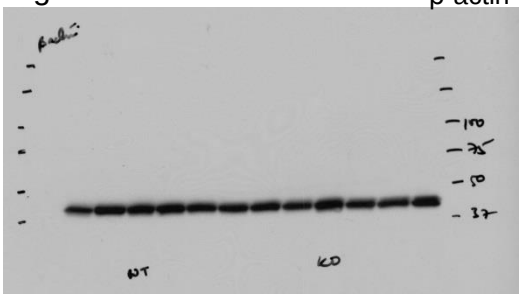

Figure 9B Glut4

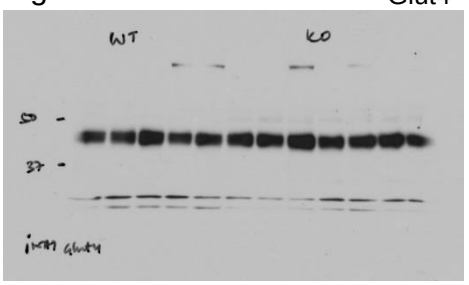

Figure 9B β-actin